



St. Joseph's Journal of Humanities and Science

ISSN: 2347 - 5331

<http://sjctnc.edu.in/6107-2/>



Sr Intercalated ZnO by Sol-gel Method and their Photocatalytic Activity

A. Vijayabalan*

T. Sri Ram

A. Amalorpavadoss

ABSTRACT

In this paper we are reported that the Sr intercalated ZnO prepared by sol-gel method. This catalyst was analyzed by powder X-ray diffraction spectroscopy, Scanning electron microscopy, Energy dispersive X-ray spectroscopy, diffuse reflectance spectroscopy and photoluminescence. The application of doped catalyst is evaluated by degradation of MB dye under visible light.

Keywords: ZnO, Methylene blue dye, visible light; Sr-ZnO

1. INTRODUCTION

Currently, organic dyes and their effluents have become some of the main sources of water pollution; these organic dyes escape from traditional wastewater treatment plants and remain in the water because of their high stability against light, temperature, chemicals, and microbial attack. Photocatalytic technique is a cheap and effective technique to solve this problem. Significant advances have recently been made in the area of semiconductor nano structures for photocatalytic applications [1-4]. One of the main advantages of the preparation of semiconductors is their effective treatment of wastewater. In the past decades, ecological problems such as air and water pollution have provided the impetus for continuous basic and applied research in the area of environmental remediation. Heterogeneous photocatalytic degradation process is an eco-friendly technique that has great potential to control aqueous organic wastes or air pollutants [5, 6]. Among a

variety of oxide semiconductor photocatalysts, ZnO is found to be a good catalyst due to its strong oxidizing power, stability, non-toxicity, chemical and biological inertness, as well as very cheap and easy of availability [7-14]. A high redox potential, a direct band-gap of 3.37eV at room temperature, a high exciton binding energy of 60 meV, superior physical and chemical stability, inexpensiveness, easy synthesis, and non-toxicity were identified as the main reasons for the wide acceptability of ZnO materials compared to the semiconductor photocatalysts. Therefore, ZnO can be used as a photocatalyst material to remove organic dyes from waste water with high efficiency [15-20]. The doping of a larger radius of Sr^{2+} ($R=2.45 \text{ \AA}$) with Zn^{2+} ($R=0.74 \text{ \AA}$) could significantly create lattice defects for the degradation of methylene blue studied by R.Yousefiet *al.*, [21]. Recently, coupled ZnO/SrO photocatalyst attract much interest in particular due to the low cost of SrO. Additionally, the band gap of SrO ($E_g = 5.5\text{-}5.9 \text{ eV}$) is higher than that of

ZnO ($E_g = 3.37$ eV), but the conduction band (CB) of SrO is lower than that of ZnO [22]. Sr-au doped zno enhanced fast degradation of AR18 dye than Sr-ZnO and Au-ZnO under UV light [23]. The crystal structures and surface properties of coupled ZnO/SrO composites were characterized by various techniques. The photocatalytic decomposition of methylene blue (MB) used as a model pollutant were investigated under visible light irradiation [24]. In this present study, the Sr-ZnO prepared by sol-gel method was characterized by several techniques and evaluated by degradation of methylene blue dye under visible light.

2. MATERIALS AND METHODS

2.1 Materials

$\text{Sr}(\text{NO}_3)_2$ (Loba-chemi), $\text{Zn}(\text{NO}_3)_2$ (Loba-chemi), MB dye (Merck) and liquid ammonia (Qualigens) were used. Distilled water is used for the makeup solution.

2.2 Methods

Preparation of Sr-ZnO by Sol-gel method

To appropriate concentration of $\text{Zn}(\text{NO}_3)_2$ and $\text{Sr}(\text{NO}_3)_2$ solution were mixed under stirring. After 1:1 aqueous ammonia solution was added to reach a pH 9.5 under continuous stirring. The catalyst are filtered, dried and calcined at 500°C for one hour in muffle furnace. The undoped ZnO are prepared by above procedure without Sr^{2+} ion.

2.3 Characterization Techniques

The powder x-ray diffraction of the sample are recorded by using a ANalyticalX'Pert PRO diffractometer with Cu Ka rays of 1.5406 \AA at 40 kV and 30 mA with a scan rate of 0.04°s^{-1} in a 2θ range of $10-75^\circ$. Scanning electron microscopes are used for analysis of morphologies of Sr-ZnO and pure ZnO by using a JSM6610 model under vacuum mode. The elemental analyses of the sample are detected by using Oxford instruments attached to scanning electron microscope (SEM). The diffuse reflectance spectra were obtained with a PerkinElmer Lamda 35 spectrometer. A PerkinElmer LS 55 fluorescence spectrometer was used to record the photoluminescence (PL) spectra at room temperature. The dye samples are analysed by HR4C2152 model UV-visible spectrophotometer.

2.4 Photocatalytic Activity

The visible light photocatalytic studies were made in an immersion type photo reactor equipped with a 150-W tungsten halogen lamp fitted into a double walled borosilicate immersion well of 40 mm outer diameter with inlet and outlet for circulation of $\text{K}_2\text{Cr}_2\text{O}_7$ solution. The 1N $\text{K}_2\text{Cr}_2\text{O}_7$ solution used removes 99 % of the UV light with wavelength between 320 and 400 nm and acts as a UV cutoff filter. After the addition of the catalyst to the dye solution, air was bubbled through the solution which kept the catalyst particles under suspension and at constant motion. The catalyst was separated after the illumination. The methylene blue dye was analyzed spectrophotometrically at 656 nm.

3. RESULTS AND DISCUSSIONS

3.1 Powder X-Ray Diffraction Spectroscopy

Fig.1 shows that the XRD pattern for the pure ZnO and Sr-ZnO. The XRD pattern of Sr-ZnO, reveals that fine diffraction peaks at (100), (002), (101), (102), (110), (103), (112) and (201) respectively, These pattern totally match with Joint Committee on Powder Diffraction Standards (JCPDS) card no. 89-1397 of hexagonal wurtzite ZnO structure [25]. The 2θ value of SrO peak at 38.25 , 44.5 and 64.73° are absent in doped catalyst. Peak shifting may be attributed to the ionic radius of the dopant Sr^{2+} ($R = 2.45 \text{ \AA}$) which is larger than that of ionic radius of Zn^{2+} ($R = 0.74 \text{ \AA}$). It is also noted that the major diffraction peaks of ZnO intensity are decreased with doped Sr [26]. The average particle size (D) is calculated from XRD values by using the Debye-Scherrer's equation $D = 0.9\lambda/\beta\cos\theta$. Where, λ is the X-ray wavelength of 1.54 \AA , β is the full-width at half maximum, θ is the Bragg's diffraction angle and surface area calculated by $S = 6/\rho D$, where S is the specific surface area, D is the average particle size and ρ is the material density. From the table-1, the crystal size of bare ZnO and Sr-ZnO are 10.08 and 10.13 nm and surface areas are 105.2 and 112.14 m^2g^{-1} respectively. It is also shows that the average particles size does not change with Sr doped compare to bare ZnO.

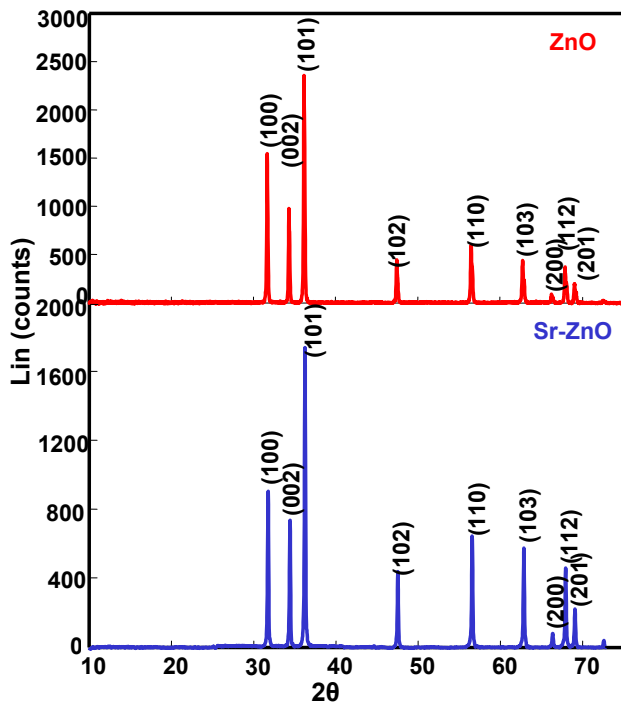


Fig.1 Powder X-ray Diffraction Spectra of Sr-ZnO and ZnO

Table-1 Crystal Size (D) and Surface Area (S) of ZnO and Sr-ZnO

Oxide	D, nm	S, m ² g ⁻¹
ZnO	10.08	105.2
Sr-ZnO	10.13	112.14

3.2 Scanning Electron Microscopy

The surface morphology of Sr-ZnO has been analysed by scanning electron microscope as shown in fig.2. It is also shows that the Sr-ZnO micron particles are agglomerated and destroy the hexagonal shape of wurtzite ZnO structures with doped Sr²⁺ion.

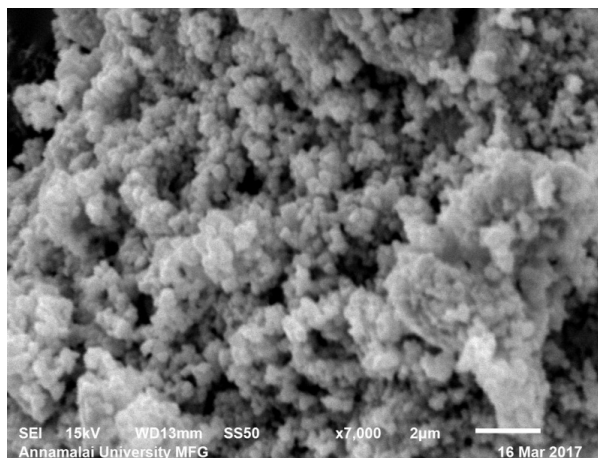


Fig.2 SEM Images of Sr-ZnO

3.3 Energy Dispersive X-ray Diffraction Spectroscopy

The energy dispersive X-ray diffraction spectrum of Sr-ZnO is shown in fig.3.. It is conclude with 1.56% Sr doped ZnO lattice.

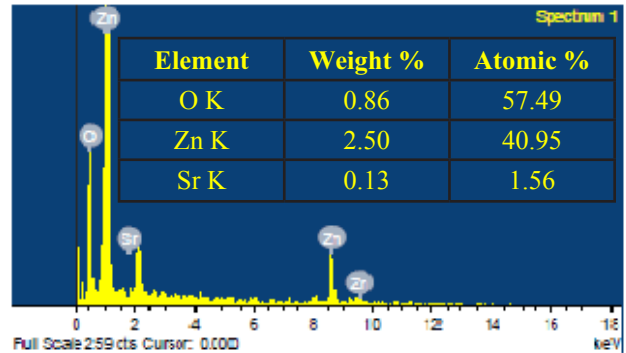


Fig.3 Energy Dispersive X-ray Spectrum of Sr-ZnO

3.4 Diffuse Reflectance Spectroscopy

The Transmittance spectrums of Sr-ZnO are shown in fig.4. In Sr-ZnO particles has higher absorption in visible region compare to bare ZnO (not shown in figure). To calculate the band gap energies of Sr-ZnO catalysts, UV-vis spectra in the diffuse reflectance mode (R) were transformed to the Kubelka–Munk function F(R) to separate the extent of light absorption from scattering. The indirect band gap energies of Sr-ZnO catalysts was obtained from the plot of the modified Kubelka–Munk function $[F(R)E]^{1/2}$ versus the energy of the absorbed light E are shown in fig.5 The indirect band gap energy of Sr-ZnO particles is 2.85eV.

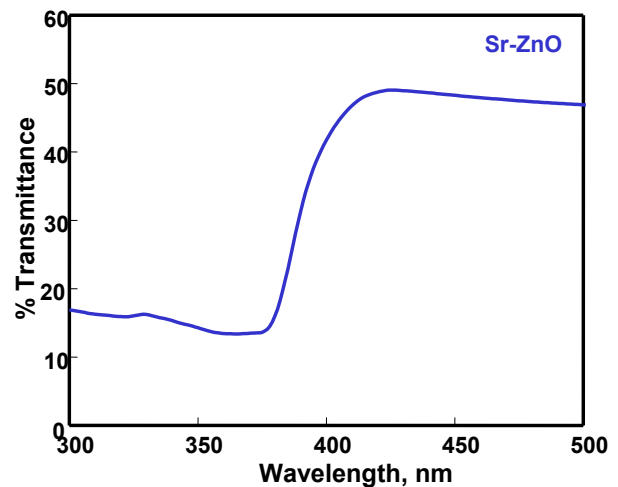


Fig.4 Transmittance Spectrum of Sr-ZnO

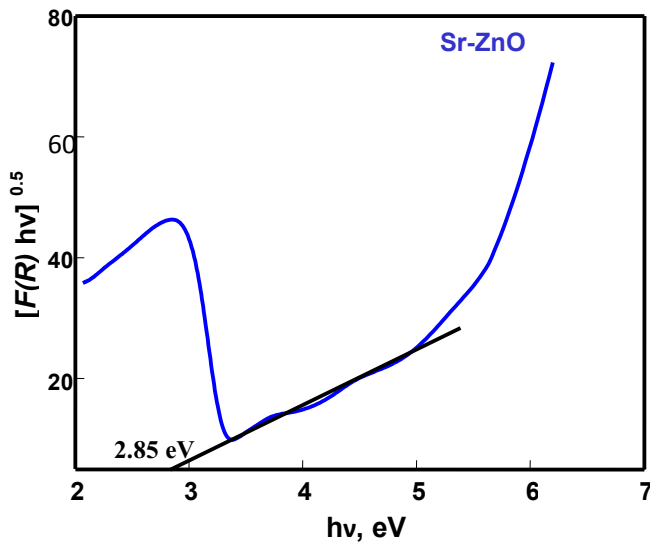


Fig.5 Tauc plot for Indirect Band Gap Energy of Sr-ZnO

3.5 Photoluminescence Spectroscopy

The photoluminescence (PL) spectra of the bare ZnO and Sr– ZnO are shown in fig.6. Photoluminescence occurs due to the recombination of electron–hole pair in the semiconductor. The loading Sr with ZnO does not shift the emission of ZnO, but the intensity of PL emission decreases when compared to bare ZnO. The trapping of photogenerated electron by Sr reduces the electron–hole recombination leading to the decrease of PL emission. This decrease in the rate of electron–hole recombination enhanced the photocatalytic activity of Sr-ZnO.

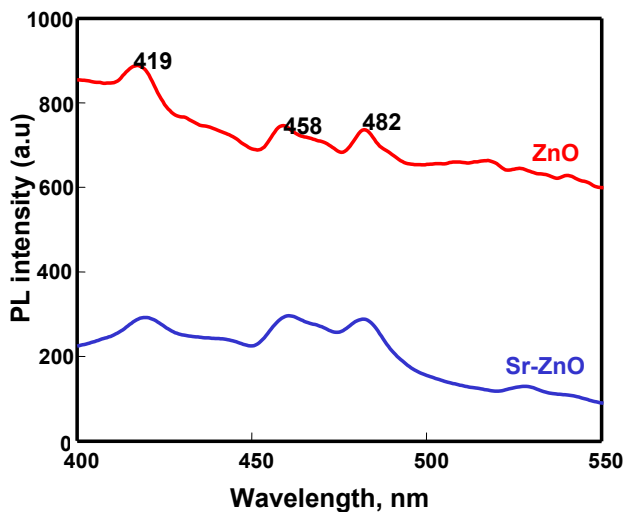


Fig.6 Photoluminescence Spectra of Sr-ZnO and ZnO

3.6 Dye Degradation

The temporal profiles degradation of methylene blue dye under visible light is shown in fig.7. The UV light active ZnO band gap energy is 3.37eV [23, 27, 28] and this value decreased due to Sr²⁺intercalated ZnO band gap energy is 2.85 eV (visible light active). It is noted that the 58% (remaining 4.3ppm dye solution) degradation is observed for Sr-ZnO in 180 min. whereas ZnO degrade 41%(remaining 6.2 ppm dye solution) in 180 min. This might be due to trapping photo-excited electrons at conduction band by decreasing the electron-hole recombination as a consequence of Sr dopant into ZnO environment. Doping has regulated the degradation occurred by exhibiting the highest photo catalytic degradation efficiency in methylene blue dye. This is because the incorporated Sr atom acts as electron traps by suppressing the recombination of photo-generated holes and electrons.

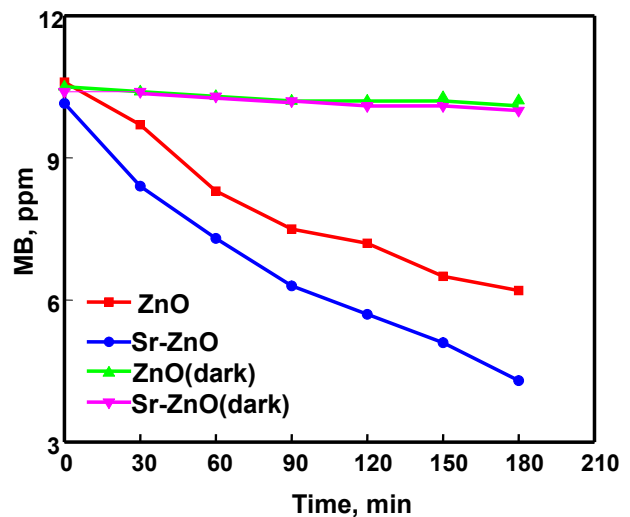


Fig.7 Temporal Profiles of Degradation of Methylene Blue Dye under Visible Light

4. CONCLUSION

The Sr doped ZnO are synthesized by sol-gel method. XRD reveals that synthesized doped ZnO are hexagonal wurtzite structure. SEM images show that the particles are agglomerated to give micron size. EDX confirms the Sr²⁺ ion present in the ZnO lattice. DRS confirm the synthesized samples are absorbed in visible region. PL reveals the emission lights are suppressed by Sr²⁺ions incorporated into ZnO lattice. Degradation of methylene blue dye is enhanced by Sr-ZnO than ZnO under visible light are due to suppression of the recombination of electron- hole pair.

REFERENCES

- [1] O. Akhavan, M. Mehrabian, K. Mirabbaszadeh, R. Azimirad, *Journal of Physics. D: Applied Physics* 42 (2009) 225-305.
- [2] A. Qurashi, Z. Zhong, M. Wakas Alam, *Solid State Science* 12 (2010) 1516.
- [3] M. Choobtashani, O. Akhavan, *Applied Surface Science* 276 (2013) 628–634.
- [4] O. Akhavan, R. Azimirad, S. Safa, E. Hasani, *Journal of Material Chemistry* 21 (2011) 9634–9640.
- [5] S. Ahmed, M.G. Rasul, W.N. Martens, R. Brown, M.A. Hashib., *Water Air Soil Pollution*. 215 (2011) 3–29.
- [6] A. Zaleska, E. Grabowska, J. Sobczak, M. Gazda, J. Hupka, *Applied Catalysis B* 89 (2009) 469–475.
- [7] B. Krishnakumar, K. Selvam, R. Velmurugan, M. Swaminathan, *Desalination of water treatment* 24(2010) 132–139.
- [8] B. Krishnakumar, M. Swaminathan, *Indian Journal of Chemical Science A* 49 (2010) 1035–1040.
- [9] R. Velmurugan, K. Selvam, B. Krishnakumar, M. Swaminathan, *Separation and Purification Technology* 80 (2011) 119–124.
- [10] Y.X. Rao, D.M. Antonelli, *Journal of Material Chemistry* 19 (2009) 1937–1944.
- [11] Y. Huang, G. Xie, S.P. Chen, S.L. Gao, *Journal of Solid State Chemistry* 184 (2011) 502–508.
- [12] Y.M. Wu, J.L. Zhang, L. Xiao, F. Chen, *Applied Catalysis B* 88 (2009) 525–532.
- [13] J.C. Yu, W. Ho, J. Yu, H. Yip, P.K. Wong, J. Zhao, *Environmental Science Technology* 39 (2005) 1175–1179.
- [14] H.J. Zhang, G.H. Chen, D.W. Bahnemann, *Journal of Material Chemistry* 19 (2009) 5089–5121.
- [15] M. Azarang, A. Shuhaimi, R. Yousefi, A. Moradi Golsheikh, M. Sookhakian, *Ceramics International* 40(2014)10217–10221.
- [16] O. Akhavan, *ACS Nano* 4 (2010) 4174–4180.
- [17] A. Nezamzadeh-Ejehieh, S. Khorsandi, *Journal Indian Engineering Chemistry* 20 (2014) 937–946.
- [18] A. Saffar-Teluri, S. Bolouk, M.H. Amini, *Research Chemical Intermediate* 39 (2013) 3345–3353.
- [19] M.A. Behnajady, Y. Tohidi, *Journal of Photochemical and Photobiology* 90 (2014) 51–56.
- [20] G. Mahmodi, S. Sharifnia, M. Madani, V. Vatanpour, *Journal of Solar Energy* 97 (2013) 186–194.
- [21] Farid Jamali-Sheini, Mohsen Cheraghizade, Sara Khosravi-Gandomani, Abdolhossein Saaedi, Nay Ming Huang, Wan Jeffrey Basirun, Majid Azarang Ramin Yousefi, *Material Science and Semiconductor Process* 32, (2015) 152–159.
- [22] T.G. Smijs, S. Pavel, *Nanotechnology Science Applied* 4(2011) 95-112.
- [23] A. Senthilraja, B. Subash, B. Krishnakumar, M. Swaminathan, M. Shanthi, *Superlattice and Microstructure* 75(2014)701-715.
- [24] S. Harish, M. Sabarinathan, J. Archana, M. Navaneethan, K.D. Nisha, S. Ponnusamy, Vinay Gupta, C. Muthamizhchelvan, D.K. Aswal, H. Ikeda, Y. Hayakawa, *Applied Surface Science* doi:10.1016/j.apsusc.2017.01.164.
- [25] C. Karunakaran, R. Dhanalakshmi and P. Gomathisankar, *Research Chemical Intermediate* 36, (2010) 361.
- [26] C. Karunakaran, “Semiconductor photoelectrocatalysis” in *Photo-Electrochemistry & Photo-Biology for the Sustainability*, Eds. S. Kaneco, B. Viswanathan, and H. Katsumata, Bentham Science Publishers, 1, 2010, pp-129.
- [27] S. Harish, M. Sabarinathan, J. Archana, M. Navaneethan, K.D. Nisha, S. Ponnusamy, Vinay Gupta, C. Muthamizhchelvan, D.K. Aswal, H. Ikeda, Y. Hayakawa, *Applied Surface Science* (2017). <http://dx.doi.org/doi:10.1016/j.apsusc.2017.01.164>.
- [28] L. Huang, Y. Hao, M. Hu, *Material Science and Semiconductor Process* 74 (2018) 303-308.